
CHAPTER: IV MAGNETISATION STUDIES

4.1 INTRODUCTION

Hysteresis studies of ferrites furnish valuable data on permeability μ . The saturation magnetisation M_s , the coercive force H_c and the remanence ratio $\frac{M_r}{M_s}$. The applicability of ferrites is due to the important data of hysteresis. The permeability values of ferrites change over wide range; therefore, ferrites are suitable for various frequency ranges.

Ferrites with low values of H_c are called as soft ferrites and they are used in the manufacture of high frequency, inductances, cores of transformers, motors and generators. These applications demand high permeability, low coercive force and small hysteresis losses of ferrites. Ferrites with high values of H_c are called as hard ferrites and they are used as permanent magnets, for various kinds of electric motors, loudspeakers, telephones, TV and other appliances which also need high remanence. In 1949 Neel has shown that the coercive force H_c is related with the crystal anisotropy the saturation magnetisation, the internal stresses and the porosity.¹

The squareness ratio determines the utility of the ferrites in the magnetic memory and switching devices. Hysteresis properties are highly dependent on chemical composition, crystal structure, porosity and grain size distribution, heat treatment and machining history² and so on. The preparation of ferrites with good squareness of loop characteristics demands most stringent conditions and atmosphere.



Maxwell described the experimental techniques for measurement of magnetic properties of ferrites. The saturation magnetisation is important basic parameter and its measurement can be made by the ballistic method, the vibration coil magnetometer, the vibrating sample magnetometer, various force methods and microwave method. We have used high field loop tracer for hysteresis studies.

4.2 Domains and Wall Formation

Weiss³ in 1907 postulated the existence of molecular field which is responsible for the spontaneous alignment of atomic magnets. However, the ferromagnetic crystals frequently exhibit the state of zero magnetisation and this fact led to the prediction of randomly oriented domains. Barkhausen⁴ in 1949 showed that the magnetisation of the specimen changes discontinuously when the applied field changes continuously. This fact supported the interpretation that the magnetisation is due to rotation of magnetisation of the whole domain. Landu and Lifshitz showed that in any ferromagnetic material domain formation results as a consequence of considerable reduction in magnetostatic energy from that of the state of saturated magnetisation.

Weiss could not explain the origin of molecular field but he stated that the interactions of magnetic moments of the electrons are too weak to explain large molecular field. Heisenberg⁵ in 1928 gave the quantum mechanical treatment for

the alignment in terms of exchange interaction between the uncompensated spins of electrons in the partially filled 3-d shells. He showed that under certain conditions the exchange energy produces effects similar to those molecular field. Electrons with parallel spins have lower energy than those with antiparallel spins. Spontaneous magnetisation can also arise as a result of negative exchange interactions under favourable conditions of intervening ions. Neel⁶ in 1948 showed that in this case, the neighbouring magnetic moments are antiparallel. This is the origin of spontaneous magnetisation in ferrites where there are magnetic moments arranged in antiparallel or some other complex fashion compensating partially. The magnetic moments contributing to the magnetisation are mainly spin magnetic moments due to the quenching of orbital angular momentum. The non-integral values of the magneton numbers in the case of Fe, Ni, Co at 0°K could not be explained by the Heisenberg model but has been explained on the basis of band theory of solids (Stoner 1933).⁷ The exchange energy is given by

$$W_{ex} = 2JS^2 \sum_{i \neq j} \cos \varphi_{ij}$$

where S is the total spin momentum per atom and φ_{ij} is the angle between the spin momentum vectors of atoms i and j.

Here anisotropy is neglected and only nearest neighbour exchange interactions are considered. The exchange energy alone would not show the observed anisotropy in the magnetic properties

of a crystal involving easy axes of magnetisation. This implies existence of an interaction between the spins and the crystal lattice. For a cubic crystal the excess energy needed to magnetise a crystal in a given direction as compared to that required for an easy direction is given by

$$W = K_1 (\alpha_1^2 \alpha_2^2 + \alpha_2^2 \alpha_3^2 + \alpha_3^2 \alpha_1^2) + K_2 \alpha_1^2 \alpha_2^2 \alpha_3^2 +$$

where K_1 and K_2 are anisotropy constants characteristic of particular material and α_1 , α_2 , α_3 are the direction cosine of magnetisation vectors with respect to the cubic axes.

When the crystal is strained there is change in the anisotropy energy which is called the magnetoelastic energy W_A . It is due to change in interatomic spacing. One more contribution to the energy is that of magnetostatic energy W_M , which is the work required to assemble all the dipoles constituting the body. The crystal is divided into domains and hence the magnetostatic energy gets reduced. This subdivision halts at a point where the energy required for the formation of additional domain wall becomes greater than the decrease in the magnetostatic energy.

Bloch⁸ in 1932 has shown that the change in the magnetisation between two neighbouring domains takes place over a finite width. If it has to occur over a unit interatomic distance very high value of exchange energy would be required. The wall of finite width contains spins whose orientations gradually change from the direction in one domain to that in the other. Thus, the

atomic spins within the wall do not remain parallel to an easy direction and so lead to some anisotropy energy. There are two types of walls. The spin rotates by 180° from one domain to other domain, it is 180° wall. In 90° , the thickness of the domain wall is determined by the condition of minimum total energy, it is given by $\delta = \left(\frac{A}{K}\right)^{1/2}$ this leads to wall energy $W_F = \frac{4}{(AK)^{1/2}}$ where A is the exchange energy constant and K is anisotropy constant.⁹ In principle the optimum domain configuration can be determined from the condition of minimum free energy i.e., by minimising.

$W = W_{ex} + W_K + W_A + W_M + W_F$ for particular value of applied field. The shape of the magnetisation curve for a crystal can be determined by repeating this procedure for the various values of applied field, but in practice it is difficult.

Bloch wall appears when there is a transition of magnetisations from a given direction to any other under the condition of zero divergence of magnetisation across the wall.

When the thickness of the specimen is small, of the order of the width of the domain wall, the interactions between the strips of free poles formed at the intersections of the wall with the specimen, surface becomes important. This was first pointed out by Neel¹⁰ in the year 1935. Neel suggested new type of transition. The wall, therefore, is called as Neel wall. Here the magnetisation rotates from one domain to the neighbouring domain while remaining in the plane of the film. In the case of

the films Neel Walls become energetically favoured. This work has been extended by Middlehoek.¹¹ In his work he suggested that the energy for different transitions is function of angles between orientations of neighbouring domains.

There is one more type of spin transitions in which the wall is called as crossed tie wall. The short right angled cross ties are regularly arranged. This structure is explained by considering the variation of the closure of flux at alternate intervals through the plane of the spin rotation around the spiraling axis of the wall. Middlehoek¹² has shown that energy of a wall of cross tie type is roughly 0.6 times the energy of Neel Wall. If the thickness of the specimen is greater than 900 \AA then Block wall is formed. If the thickness of the specimen is less than 900 \AA then cross the wall is formed.

According to these theoretical considerations Neel Wall is not expected to be formed at all.

However, in specimens of thickness less than about 200 \AA Neel walls are observed.

Experimental results deduct the formation of more complex walls, where spin rotations are complex. Such walls may consist of alternate sections of pure Bloch type of transitions and pure Neel type transitions. In between the two regions a region of complex combination is present.

If the material is polycrystalline, with grains not very

small, the domain structure for each grain is roughly similar to those in large crystals. Due to small dimensions of the grains and due to interaction between adjacent grains, modification in the domains takes place. Results in the case of polycrystalline ferrites are similar to those observed for single crystals.

4.3 Irreversibility and Hysteresis

Irreversibility and hysteresis in ferromagnetic materials are attributed to impediments to the motion of domain walls offered by defects like inclusion, heterogeneties due to other phase and dislocations.¹³ If applied magnetic field is small, the magnetisation proceeds by reversible wall motion. If the field is greater than threshold value magnetisation takes place by irreversible wall motion and at very high fields irreversible wall rotations. Above the threshold field, Barkhausen jumps are observed in magnetisation and wall energy is maximum. This leads to irreversible increase in magnetostatic and magnetoelastic energies of the material under the action of external magnetic field. When the magnetic field is reduced to zero, the residual magnetisation remains locked, the thermal energy required for randomisation and wall motion not being available. Also during magnetisation reversal nucleation has to proceed before the sequence of reversible and irreversible wall motion and spin rotation can take place. Therefore, for a unisolated specimen the changes result in hysteresis during the magnetisation cycle.

signifying the energy loss. Keroten¹⁴ in 1943 proposed the model of wall motion, for inhomogenous material having nonmagnetic inclusion considers changes in the energy of the domain wall due to variations of the area of the wall.

The strain and the inclusion theories considered only plane domain walls and regular arrays of imperfections and also did not deal with the magnetic disturbances created by the imperfections. However, in view of the statistically distributed imperfections, the number of imperfections that will not be intersected by the wall on an average would remain the same. Further Neel established that there are variations in magnitude and direction of magnetisation due to randomly distributed irregularities within the same domain. From this dispersed field theory Neel calculated critical field required for irreversible moments of domain wall and coercivity.

Goodenough¹⁵ in 1954 has presented in detail the nucleation centres of reverse domains in a saturated polycrystalline specimen considering the magnetostatic energy associated with the defects. He examined the effects of granular inclusions, lamellar precipitates, grain boundaries and the crystal surface and arrived at the conclusion that these are most likely centres of reverse domain formation. When a magnetic material consists of fine particles likely to be single domain, the process of magnetisation reversal can only take place by rotation through the hard directions with consequent irreversibility. The studies

on the coercivity of the sample having single domain particles with uniaxial anisotropy imbedded in a matrix showed that the demagnetising fields of the particles themselves determine the coercivity.¹⁶ However, Stoner and Wohlfarth's calculations of coercivity do not agree with the values reached in practice. This can be partly explained by the magnetic interactions between the particles and the possibility of other mechanisms of magnetisation reversal like fanning reversal mechanism, incoherent spin rotation by magnetisation bulking and magnetisation curling.¹⁷

4.4 Losses

When alternating magnetic fields is applied on the magnetic material the part of magnetic energy is absorbed by the material and dissipated as heat. If alternating magnetic field is expressed as $H = H_0 \exp(i\omega t)$, then the induction B can be represented as $B = B_0 \exp[i(\omega t + \delta)]$ so that

$$\begin{aligned} \mu &= \frac{B}{H} = \frac{B_0}{H(\cos\delta + i\sin\delta)} \\ &= \mu' + i\mu'' \end{aligned}$$

where μ' gives that component of the flux which is in phase, and μ'' the one that is 90° out of phase with the applied field. The energy loss is proportional to μ'' . The ratio $\frac{\mu''}{\mu'} = \tan\delta$ is called as power factor or loss factor. The quality factor

$$Q = \frac{\mu'}{\mu''} = \frac{1}{\tan\delta}$$

from the point of view of applications the variation of μ' and μ'' against frequency is an important criterion and is called as permeability spectrum.

The important mechanisms of losses are (1) hysteresis, (2) eddy currents, (3) spin resonance, (4) relaxation and wall resonance. If applied magnetic field on ferrites hysteresis and eddy current losses are very small, and the major contribution comes from the remaining sources.

4.4.1 Hysteresis losses

The energy dE required to change magnetisation M to $M+dM$ at a field H is given by $dE = HdM$. Total energy absorbed for a complete hysteresis cycle is $W = \oint HdM$. This is equal to area of bounded by hysteresis loop. Low coercivity or high permeability results in a small area under the loop and hence a small loss.

4.4.2 Eddy Current Loss

An electric current is induced in the magnetic core material by the alternating magnetic field. Heat is evolved and loss of power takes place. Power loss per second is proportional to F^2/ξ , where F is the frequency and ξ the electrical resistivity of the core material, the constant of proportionality depends upon geometry of the core.

4.4.3 Spin Resonance Loss

Under the influence of internal anisotropy field H_k , the electron spin vector in a magnetic material precesses with frequency ω given by $\omega = rH_k$, where r is the gyromagnetic ratio. If electron spin vector is subjected to an external r-f magnetic field H_1 in a direction perpendicular to that of H_k , then resonance sets in when the radio frequency matches the precessional frequency and energy is absorbed from applied field. In case of a material with negative crystal anisotropy constant the rotational processes are important, then the resonant frequency is inversely proportional to (μ) . Therefore, when the permeability of the material is higher the resonant frequency is lower.

4.4.4 Relaxation Loss

Due to exchange between Fe^{2+} and Fe^{3+} ions relaxation losses take place. As magnetisation changes direction, then Fe^{2+} and Fe^{3+} ions tend to change their position to attain the configuration that has lower energy under the changed direction of magnetisation. The readjustment of the Fe^{3+} , Fe^{2+} positions does not require movement of ions, but merely that of electrons.

The loss depends upon frequency and is maximum when the applied frequency is close to the relaxation frequency for electron jump for a given material at a given temperature.

4.4.5 Wall Resonance Loss

In certain samples, the low frequency loss has been identified as due to domain wall resonance. If the domain wall is disturbed from its equilibrium position, restoring force sets in, which tries to bring back. The wall, like a stretched membrane, thus has a natural frequency of oscillation. If the frequency of applied magnetic field matches this natural frequency, resonance absorption sets in.

4.5 Measurement Procedure

The measurement of M_s , M_r and H_c were carried out on the screen of oscilloscope illuminated adequately. Standard Ni-sample having saturation magnetisation of 53.34 emu/gram was used for the calibration of the screen when the current through the coil of the magnet was 180 mA. Hysteresis loop was obtained on the CRO screen with the help of controls provided. The signal from the balancing coil after integration is proportional to the magnetic moment, of the specimen fed to vertical plates of the oscilloscope after suitable amplification. A signal proportional to magnetic field is fed to the horizontal plates of CRO. Thus oscilloscope displays magnetic moment V_g field that is the hysteresis loop of the sample. Without disturbing controls of high field loop tracer and CRO, the samples of $Zn_xMg_{1-x}Fe_2O_4$ were introduced into C core, of the magnet and hysteresis loop was observed for each sample for the measurement of M_r , M_s and H_c . The high field loop tracer operates on 230 voH, 50 Hz A.C.

4.6 Results and Discussion

In figure 4.1. compositional variation of n_B has been shown for the ferrite $Zn_xMg_{1-x}Fe_2O_4$. The variation indicated by circled points is for slow cooled samples, while that indicated with traingled points is for the samples quenched from $800^{\circ}C$. The nature of variation exhibited by both these series of sample is similar. It is seen that as the content of zinc in the ferrite $Zn_xMg_{1-x}Fe_2O_4$ system is increase the values of n_B show an increasing trend up to content of zinc corresponding to value of $X=0.4$. For the content of zinc beyond the value of $X=.4$, decreasing trend is exhibited by compositional variation of n_B . The values of n_B are minimum for samples of $MgFe_2O_4$ and $Mg_{.4}Zn_{.6}Fe_2O_4$; while the value of n_B is maximum for the sample $Mg_{.6}Zn_{.4}Fe_2O_4$.

In figure 4.2 compositional variation of M_s ($\frac{emu}{gram}$) fo the slow cooled and the quenched samples of $Zn_xMg_{1-x}Fe_2O_4$ is shown.

In table 4.1, we have also given Y-K angles for our system. Srivastava et al¹⁸ have calculated the Y-K angles in $Zn_xFe_{3-x}O_4$. R.G. Kulkarni et al¹⁹ have carried out studies on magnetic odering in Cu-Zn ferrite. They have calculated theorgtical values of Y-K angles using the formula

$$\cos YK = \frac{5(1-x)^2 \alpha + 25(1-x^2) \beta}{(1-x^2) + 25(1+x^2) + 10(1-x^2) 6}$$

They have used the values of exchange constents as given--

$$J_{\alpha} = -5.25, J_{\beta} = -14.8, J_{\delta} = -10, J_{\gamma} = 389, J_{\epsilon} = -4.53$$

which are calculated by Srivastava et al. They have compared the theoretical values of Y-K angles with those of experimental values and concluded that canted type of spins are favoured on B sublattice in the case of CuZn ferrite. We have used the following formula for the calculation of Y-K angles:

$$n_B = (6+x) \cos \alpha_{YK} - 5(1-x)$$

where n_B is expressed in the units of Bohr magneton and x represents content of zinc. The experimental values of magnetic moment were obtained using the formula²⁰

$$n_B = \frac{\text{Molecular Weight} \times M_s}{5585 \times d_s}$$

where d_s = density of sample. σ_s = saturation magnetisation in emu per gram. M_s was calculated as follows:

$$M_s = (1-p) \sigma_s d_s; \text{ where } p \text{ is porosity.}$$

From Table 4.1 it is seen that the Y-K angles for $MgFe_2O_4$ and $Mg_{.8}Zn_{.2}Fe_2O_4$ in case of both slow cooled and quenched samples are zero. This is indicative of the fact that the magnetisation variation for these samples can be explained on the basis of Neel two sublattice model. The cation distribution can be represented as $(Zn_x^{2+} Fe_{1-x}^{3+})^A (Fe_{1+x}^{3+} Mg_{1-x}^{2+})^B O_4$. This cation distribution is presented on the basis that the non-magnetic Zn^{+2} ion has a strong preference for the A-site.²¹ When it goes to A-site to replace equal number Fe^{+3} ions which then occupy B-site. $MgFe_2O_4$ is partly inverted, however, Mg has a strong

preference for B-site. The net magnetic moment per formula unit therefore can be given as

$$n_B = [5(1+x) + m(1-x) - 5(1-x)] \text{ Bohr magneton}$$

where M is the magnetic moment of Mg^{+2} ions in Bohr magnetons.

It is seen that n_B should be minimum equal to M for $x = 0$, for $MgFe_2O_4$ and tend to 10 as the content of zinc is increased. However, this value of n_B is never realised in practice. From Fig. 4.2 it is seen that the value of M_s and hence n_B goes on decreasing beyond 40 per cent of content of zinc.

For the ferrites $Mg_{.6}Zn_{.4}Fe_2O_4$ and $Mg_{.4}Zn_{.6}Fe_2O_4$ it is seen that Y-K angles are nonzero for both the slow cooled and the quenched samples. This suggests that for these two samples Neel two sublattice model is not applicable to explain the compositional variation of M_s . It is further seen that as the content of zinc is increased Y-K angles also increase. Thus the change in the magnetisation on the substitution of zinc occurs due to presence of Y-K angles in spin system on B site. The condition for Y-K angles to occur in NiZn system has been investigated in the molecular field approximation by Satyamurthy *et al.*,¹⁸ using a non-colinear three sublattice model. The increase in Y-K angles indicates the increasing favouring of triangular spin arrangement on B-sites leading to reduction in A-B interaction. B-B interactions are antiferromagnetic even in a mixed magnetic zinc ferrite. The effect of B-B interaction is usually masked by

strong A-B interaction which causes the spin on B-sites to be aligned parallel to each other. However, the substitution of zinc in excess of 20 per cent leads to canted type of arrangements on B-sites weakening the A-B interaction as suggested by Yafet and Kittle.²²

For the samples of $Mg_{.2}Zn_{.8}Fe_2O_4$ and $ZnFe_2O_4$ the values of M_s were found to be zero giving $\alpha_{yk} = 90^\circ$ suggesting that B-B interactions collapse when Zn is added in excess of 60 to 70 per cent.

The values of n_B for the samples of $Zn_xMg_{1-x}Fe_2O_4$ system quenched from $800^\circ C$ are found to be higher than those of the slow cooled samples. $CuFe_2O_4$ and $MgFe_2O_4$ are sensitive to heat treatment and are partially inverted ferrites.²² When ferrites containing Mg or Cu are quenched from elevated temperatures the cation distribution whatever at that temperature will be frozen in. There is a cation migration (Mg^{+2} or Cu^{+2}) from B-site to A-site. More the temperature of quenching more is this cation migration leading to higher values of n_B . In case of ferrites with Y-K angles 0, Neel's two sublattice model is valid for the quenched samples for the ferrites with nonzero α_{yk} , it is seen that on quenching Yk angles are lowered. This reduction α_{yk} angles suggests strengthening of AB interaction on quenching thereby elevating the values of n_B . This fact is corroborated by the compositional variation of T_C . The T_C values show decrease on quenching. This behaviour is similar to the compositional

variation of T_c reported earlier.²³

Figure 4.4 shows compositional variation of $\frac{M_r}{M_s}$. It is seen that in case of slow cooled samples of $Zn_xMg_{1-x}Fe_2O_4$ as the content of zinc is increased $\frac{M_r}{M_s}$ shows monotonic decrease. The value of $\frac{M_r}{M_s}$ is maximum for $MgFe_2O_4$ and minimum for $Zn_{.6}Mg_{.4}Fe_2O_4$. However, a very interesting trend is exhibited by a compositional variation of $\frac{M_r}{M_s}$ by the samples of $Zn_xMg_{1-x}Fe_2O_4$ quenched from $800^\circ C$. The value of $\frac{M_r}{M_s}$ goes on increasing as the content of zinc is increased upto the value of $x = 0.4$ and decrease thereafter for $x > 0.4$

The decrease in the value of $\frac{M_r}{M_s}$ with addition of zinc indicates more increase in M_s than that in M_r . In addition to this $\frac{M_r}{M_s}$ depends upon the factors like impurities, defects, polarizable constituents and other hinderances to domain wall motion, which determines retentivity. Thus in case of slow cooled ferrites the hinderances to domain wall motion tend to increase with the addition of zinc. However, in case of quenched samples hinderances to the domain wall motion appeared to be annealed out to their equilibrium concentration and hence are present in less degree in the samples quenched from $800^\circ C$. This may be because defects clusters are less favoured; at high temperature. Hence $\frac{M_r}{M_s}$ show increase with the addition of zinc in the quenched samples of $Zn_xMg_{1-x}Fe_2O_4$ from $x = 0$ to $x = 0.4$. However, the sample $Zn_{.6}Mg_{.4}Fe_2O_4$ shows lower value of $\frac{M_r}{M_s}$.

This may be attributed to the magnetic ordering change that occurs in the zinc substituted ferrites when content of zinc exceeds 50 per cent.

Table 4.1: Saturation magnetisation, remanent magnetisation, squareness ratio Yafetkittle angles and magnetic moment per formula unit.

History of samples slow cooled samples	M_s $\frac{\text{emu}}{\text{gram}}$	M_r $\frac{\text{emu}}{\text{gram}}$	$\frac{M_r}{M_s}$	α_{YK} in degree	$n\beta$ Bohr magneton	T_c in $^{\circ}\text{C}$
MgFe_2O_4	27.95	22.35	0.8	0°	1.00	482
$\text{Mg}_{.8}\text{Zn}_{.2}\text{Fe}_2\text{O}_4$	59.8	44.87	0.75	0°	2.23	375
$\text{Mg}_{.6}\text{Zn}_{.4}\text{Fe}_2\text{O}_4$	64.61	42.5	0.66	30.75°	2.50	282
$\text{Mg}_{.4}\text{Zn}_{.6}\text{Fe}_2\text{O}_4$	16.8	10.6	0.63	66.08°	0.68	145
$\text{Mg}_{.2}\text{Zn}_{.8}\text{Fe}_2\text{O}_4$	0	0	-	90°	-	-
ZnFe_2O_4	0	0	-	90°	-	-
Quenched from 800°C						
MgFe_2O_4	32.30	23.48	0.73	0°	1.16	435
$\text{Mg}_{.8}\text{Zn}_{.2}\text{Fe}_2\text{O}_4$	65.27	47.92	0.76	0°	2.43	340
$\text{Mg}_{.6}\text{Zn}_{.4}\text{Fe}_2\text{O}_4$	70.2	56.14	0.80	26.65°	2.72	245
$\text{Mg}_{.4}\text{Zn}_{.6}\text{Fe}_2\text{O}_4$	19.61	11.20	0.57	54.99°	0.30	120
$\text{Mg}_{.2}\text{Zn}_{.8}\text{Fe}_2\text{O}_4$	0	0	-	90°	-	-
ZnFe_2O_4	0	0	-	90°	-	-

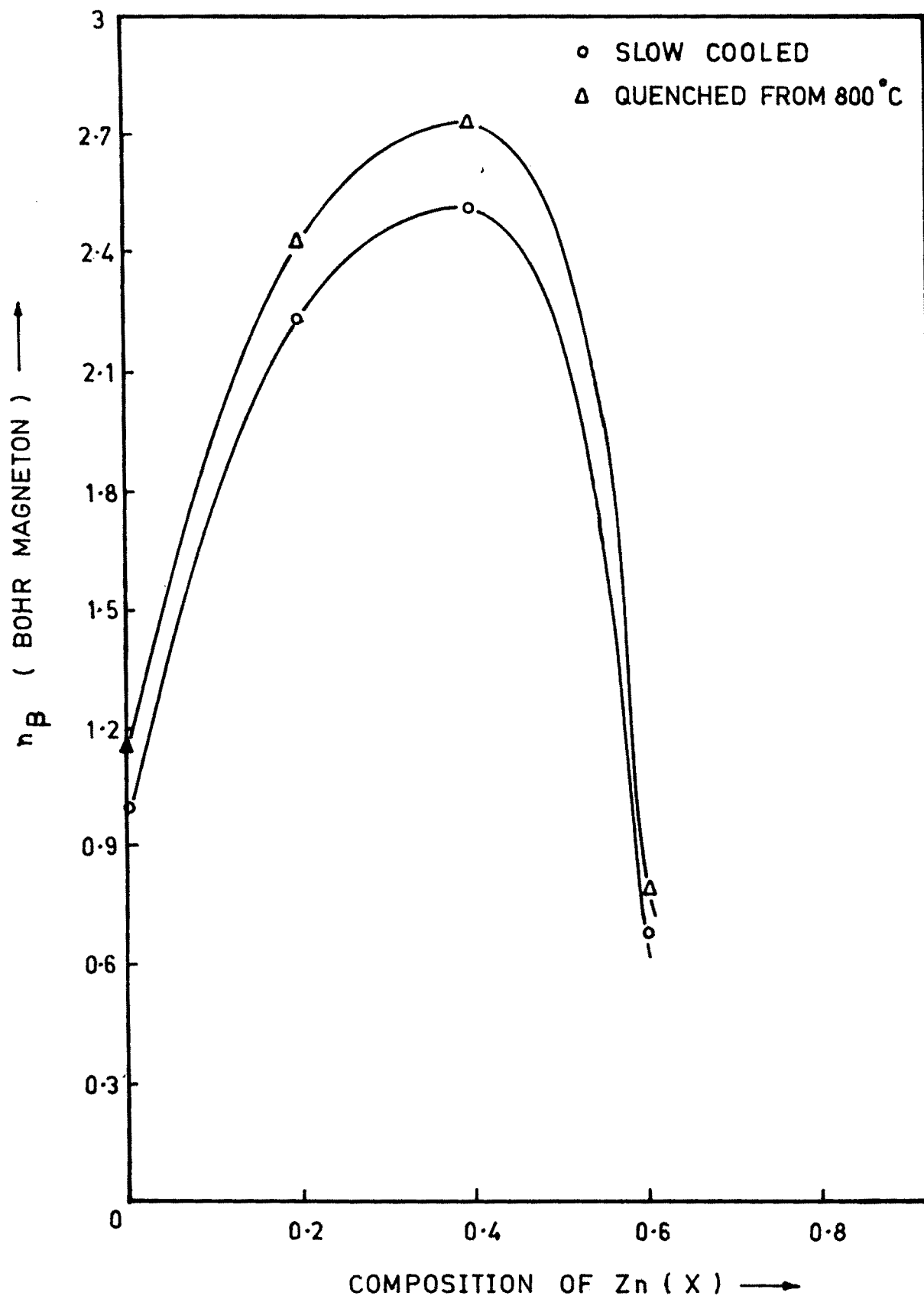


Fig. 4-1

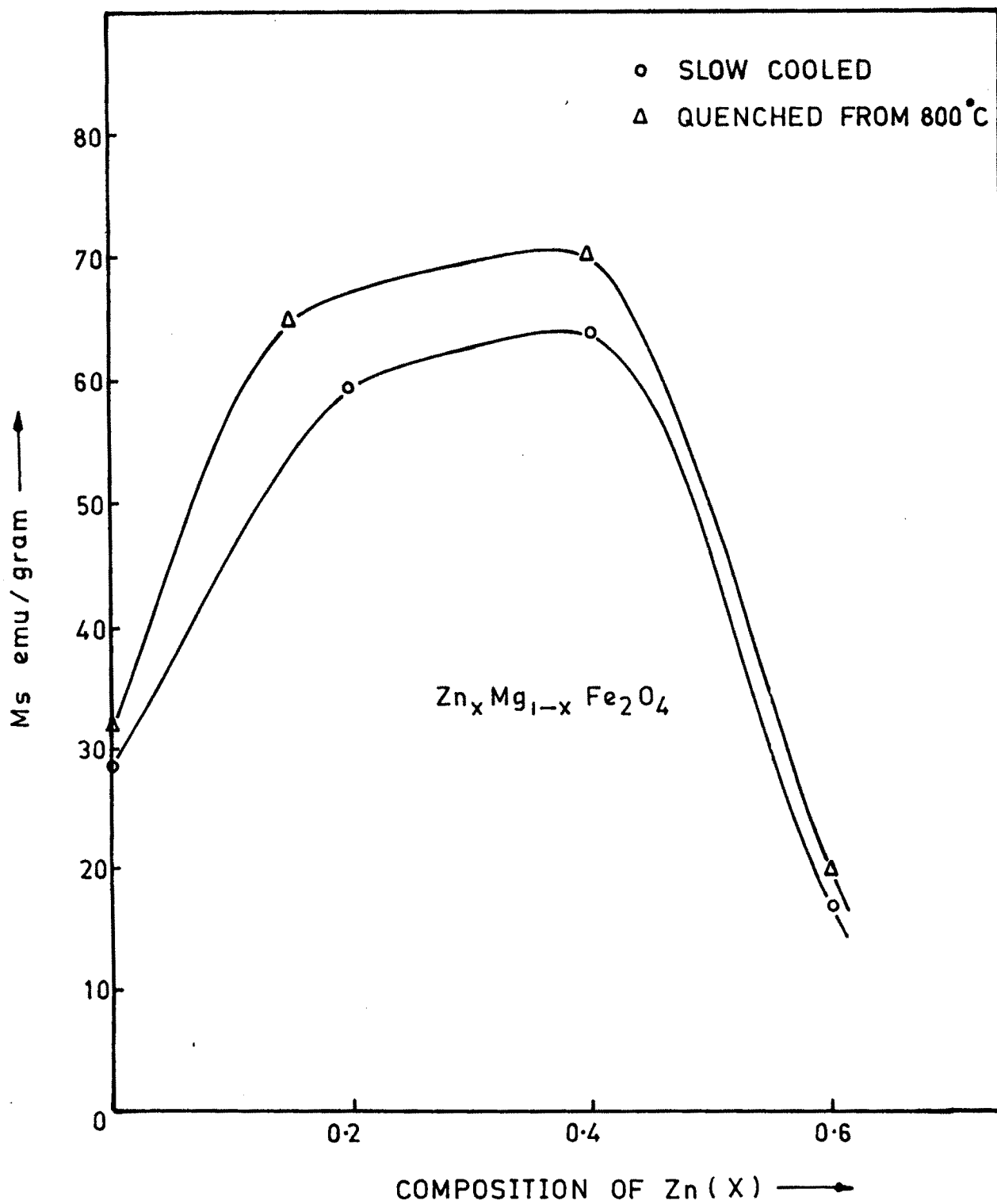


Fig. 4.2

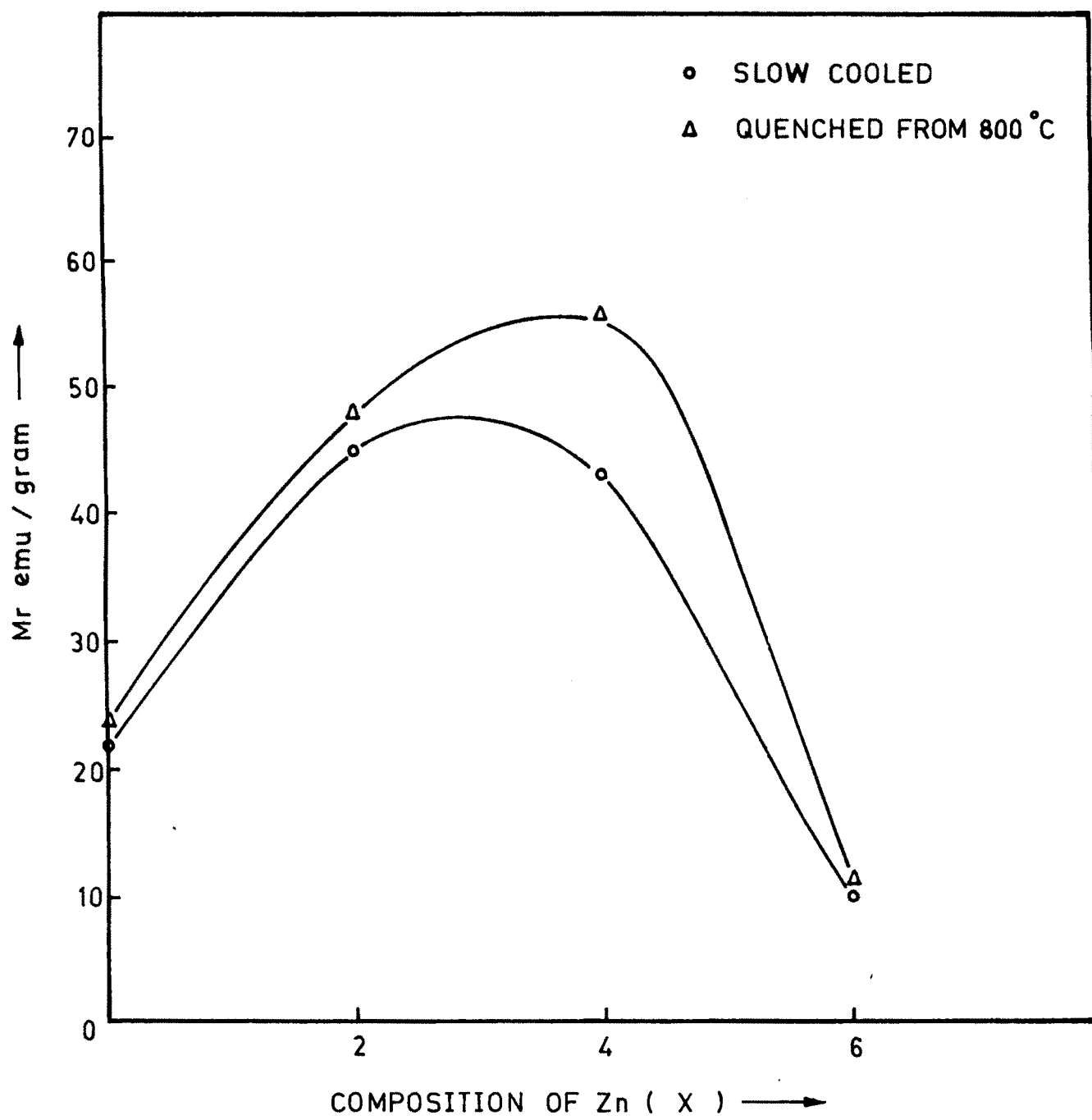


Fig. 4.3

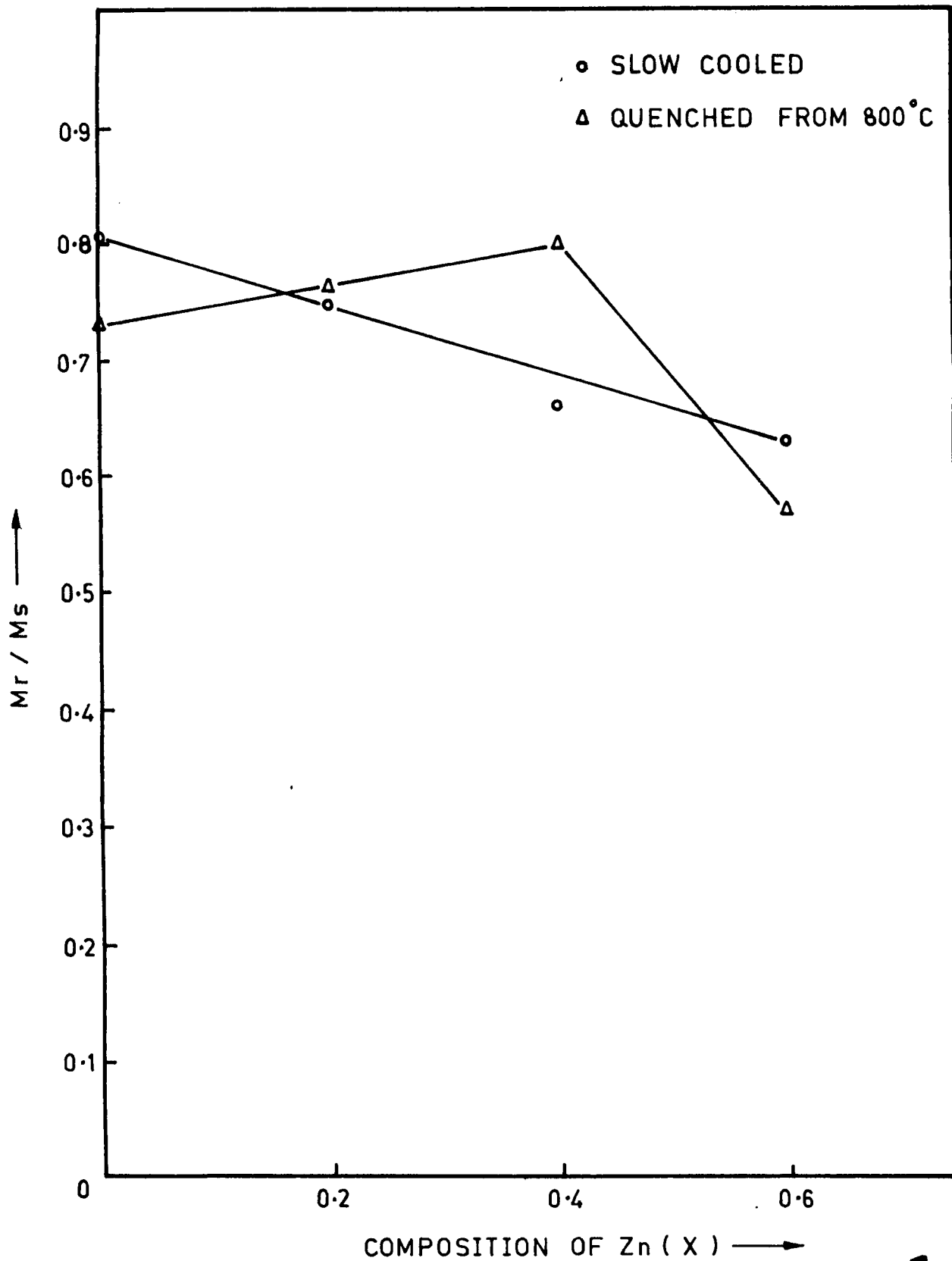


Fig. 4.4

NOTES AND REFERENCES

- 1 Alper, A.M. 'High temperature oxides' Academic Press N.Y. (1971).
- 2 Stern E. Microwave materials and applications, Jr. Appl. Phys. Vol. 38 No. 3(1967) pp. 1397-99.
- 3 Weiss, P. "L hypothese du champ molecularie et la propiete Ferromagnetique" J. de Physique, 6 (1907), p. 661.
- 4 Barkhausen, H. "Two phenomenon uncovered with the help of new amplifiers" Phys. Zeits, 20 (1919), p. 401.
- 5 Heisenberg, W. "On the theory of Ferromagnetism Zent fur Phys., 49 (1928), p. 619.
- 6 Neel L., Magnetic properties of Ferrites, ferromagnetism and antiferromagnetism", Ann Physique 3, 1948, p. 137.
- 7 Stoner, E.C., "Atomic moments in Ferromagnetic metals and alloys with non-ferromagnetic elements", Phil. Mag., 15, (1933), p. 1018.
- 8 Bloch, F., "Theory of exchange problem and residual ferromagnetism", Zeit fur Phys. 74, 1932, p. 295.
- 9 Sinha, A.P.B. and Menon, P.G., Solid State Chemistry Marcel Dekker, Inc. N.Y. (1974).
- 10 Neel, L., "Energie des puros de Bloch dans les couches minces", compt. Rend. Acad. Sci. Paris, 241 (1955), p. 533.

- 11 R. Carry and E.D. Issac, *Magnetic Domains and Techniques for their observation*, The English Uni. Press Ltd., London E.C. 4 (1966).
- 12 Middehoek, S., "Domain Walls in their Ni-Fe films", *J. Appl. Phys.*, 34 (1963) p. 1054.
- 13 Kondorsky E., "On the nature of the coercive force and irreversible changes in magnetisation", *Physik Z. Sowjetunion*, 11 (1937), p. 597.
- 14 Keroten, M., "Grundlagen Ciner Theories der ferromagnetischen Hysereise and der Kuerzitivkraft, Hirzel Leipzig (1943).
- 15 Goodenough, J.B. "A theory of domain creation and coersive force if Polycrystalline ferromagnetics, *Phys. Rev.* Vol. 95, No. 4, Aug. 15 (1954), pp. 917-932.
- 16 Stoner E.C. and Wohlfarth E.P., "Interpretation of high coercivity in ferromagnetic material, *Nature* 160 (1947) p. 650.
- 17 Frei, E.H., Shtrikman, S. and Treves, D., "Critical Size and Nucleation field of ideal ferromagnetic particles" *Phys Rev.*, 106 (1957), p. 446.
- 18 N.S. Satyamurthy, M.G. Netera, S.I. Youssef, R.J. Begum and C.M. Shrivastava, *Physical Review*, 181 (1969) p. 969.
- 19 R.G. Kulkarni, *Magnetic Ordering in Cu-Zn Ferrite*, *Jr. Mat. Sc.*, 17 (1982), pp. 843-848.

- 20 K. Sheshan, A.L. Shashimohan, D.K. Chakrabarti, A.B. Biswas, "Cation distribution and magnetic properties of Ni-MgFe₂O₄ system", N.P.S.S.P. Symposium.
- 21 Guillaud, Magnetic properties of Ferrites, J. Phys. Rad., 12 (1951), pp. 239-248.
- 22 P.J.B. Clarricoats; Microwave ferrites, London Chapman and Hall (1961).
- 23 S.R. Sawant and R.N. Patil. Structural and lattice parameter changes in the slow cooled and quenched Cu_xZn_{1-x}Fe₂O₄ samples, J. Mater Sci. 16 (1981), pp. 3496-3499.